

Muscle activity and hydrodynamic function of pelvic fins in trout (*Oncorhynchus mykiss*)

E. M. Standen

Museum of Comparative Zoology, Harvard University, 26 Oxford Street, Cambridge, MA 02138, USA
 em.standen@post.harvard.edu

Accepted 19 November 2009

SUMMARY

Contrary to the previous premise that pelvic fins lacked obvious function, recent work on three-dimensional fin motions suggests that pelvic fins actively control stability and speed in slowly swimming trout. This study used electromyography to measure pelvic fin muscle activity and particle imaging velocimetry to quantify flow along the ventral body region to test this hypothesis. Fish swam at slow speeds ($0.13\text{--}1.36\text{ BL s}^{-1}$) while being filmed with three high speed cameras. Three-dimensional kinematics were captured for all trials. During EMG trials pelvic fin muscle activity was synchronized to kinematic motion, during particle imaging velocimetry trials, a laser light-sheet was used to visualize the flow surrounding the ventral aspect of the fish. Four main conclusions are reached: first, pelvic fins are actively oscillated during slow-speed swimming; antagonistic abductor and adductor muscles contracted simultaneously, their collective action producing a unique contralateral oscillating behaviour in the fins. Second, pelvic fins slow the flow along the ventral side affecting pitch and yaw instabilities; flow upstream of the pelvic fins is slowed by 0.02 m s^{-1} and flow downstream of the pelvic fins is slowed by 0.034 m s^{-1} compared with free stream flow. Third, pelvic fin wake influences anal fin angle of attack; flow angle in the wake of the pelvic fin was $33.84\pm 2.4\text{ deg. (max)}$ and $-11.83\pm 1.2\text{ deg. (min)}$ compared with the free stream flow angle of $1.27\pm 0.1\text{ deg.}$ Fourth, pelvic fins appear to actively damp body oscillation during slow-speed swimming, providing drag to help control speed and stabilize the body position during slow-speed swimming.

Key words: electromyography, hydrodynamics, swimming, manoeuvring, pelvic fin, evolutionary fin function, stability, trout, *Oncorhynchus mykiss*.

INTRODUCTION

Recent interest in the paired pectoral fins, and median dorsal, anal and caudal fins have established the understanding that fins produce forces important for thrust production and stabilization during swimming (Drucker and Lauder, 2005; Hale et al., 2006; Peng et al., 2007; Tytell et al., 2008). Until recently the pelvic fins have not been included in the modern literature on fish swimming. This paper attempts to test hypotheses that were recently proposed about the complex three-dimensional motion of pelvic fins (Standen, 2008).

Although there has been documentation of derived species of fish such as the carpet sharks (Hemiscylliidae), skates and rays (Batoidea), frog fishes (Antennariidae) and searobins (Triglidae) using highly modified pelvic fins for ground based locomotion punting and walking along the sea floor, very little has been published (Pridmore, 1994; Pridmore, 1995; Goto et al., 1999; Wilga and Lauder, 2004). Early work that focused on pelvic fins used for locomotion in the water column suggested they had extremely limited function during swimming (Monoyer, 1866; Grenholm, 1923; Harris, 1937; Harris, 1938). Standen challenged this notion by completing a kinematic analysis of pelvic fin motion in slowly swimming trout (Standen, 2008). The three-dimensional contralateral oscillation of the pelvic fins that was described established a series of testable hypotheses regarding the activity and hydrodynamic function of pelvic fins when used at slow speeds. The first hypothesis proposed that because motion of the fins appeared to be against local flow direction, the fins must be actively controlled by their intrinsic musculature. Second, the abduction of the fins throughout their oscillation cycle would produce drag,

slowing the forward velocity of the fish. Third, the pronation and supination of the fins relative to their mid-sagittal plane would produce lateral jets and act to dampen body oscillation during slow-speed swimming.

This paper tests these three main hypotheses (Standen, 2008). Eliciting the same behaviour of slow steady swimming as in the previous study, electromyography was used to measure the muscle activity of the intrinsic fin musculature of pelvic fins in slowly swimming trout. Particle imaging velocimetry (PIV) was also used to visualize flow conditions surrounding the pelvic fins to help clarify their hydrodynamic function. Finally, by visualizing flow along the entire belly of the fish, this paper is the first to include a full body analysis of fin wakes and how they influence ventral flow in swimming fish.

MATERIALS AND METHODS

Fish

Data were collected using nine rainbow trout (*Oncorhynchus mykiss* Walbaum 1792) raised at Blue Stream Hatchery, West Barnstable, MA, USA in natural bottom stream channels. Fish were maintained in the laboratory in a 12001 circulating tank and kept on a 12 h:12 h L:D photoperiod with a mean water temperature of 16°C ($\pm 1^{\circ}\text{C}$). The nine individuals analyzed in this study had a mean total body length of 21.9 cm [range 18.5–26.9 cm; standard error of the mean (s.e.m.)=1.12] and a mean total mass of 109.8 g (range 59.1–165.4 g; s.e.m.=14.64 g). All experiments were conducted in accordance with Harvard University IACUC guidelines under protocol #20-03 to George Lauder.

Behavioural observations

Electromyography (EMG) data and hydrodynamic data could not be collected simultaneously because of electrical interference produced by the lasers used during PIV. PIV and EMG experiments were conducted sequentially.

During electromyographic experiments trout swam in the centre of the working area (28 cm wide, 28 cm deep, 80 cm long) of a variable speed flow tank under conditions similar to those described previously (Standen, 2008). Fish were recorded swimming steadily at speeds from 0.21 to 0.96 $BL s^{-1}$ (body lengths per second). Steady swimming consisted of constant tailbeating and fin oscillation. Fish were swum at slow speeds to elicit pelvic fin oscillations; at higher speeds pelvic fins are tucked against the body and not oscillated. These are relatively slow speeds for trout, their critical swimming speed, or the speed at which they can swim for 45 min before exhaustion is 1.73–2.0 $BL s^{-1}$ (Webb, 1971a; Webb, 1971b) Studies of tagged fish in pens have shown their preferred swimming speed to be between 0.48 and 0.58 $BL s^{-1}$ (Webb, 1971a; Webb, 1971b; Kawabe et al., 2003). Fish also performed yawing manoeuvres while swimming at speeds from 0.21 to 0.84 $BL s^{-1}$. Manoeuvres were not elicited but occurred as spontaneous feeding behaviours as fish foraged for particles in the flow tank. Two roughly orthogonal synchronized high-speed video cameras (Photron Fastcam 1024 PCI, 1024×1024 pixels) were used, operating at 250 frames s^{-1} (1/250 s shutter speed) to visualize the movement patterns of the pelvic fins (Fig. 1).

During hydrodynamic experiments trout swam in exactly the same set up as described above with the addition of a third synchronized ventral high-speed camera to visualize the laser light sheet transected by the pelvic fins. Lens filters were placed on each camera to facilitate the simultaneous collection of kinematic and laser light sheet data. Lateral and ventral light video cameras were fitted with blocking lens filters (CVI CG-OG-550-2.0-2.5, CVI Melles Griot, Rochester, NY, USA) which reduced the transmission of argon laser light, and resultant glare. Also, the ventral PIV camera was fitted with a transmission lens filter that let in only the laser light reflecting off the particles in suspension (CVI F10-514.5 4-2.00, CVI Melles Griot), removing the light required for kinematic filming. For clearer analysis of the PIV images synchronized cameras were operated at 500 frames s^{-1} and fish were recorded swimming steadily at speeds from 0.13 to 1.36 $BL s^{-1}$. The difficulty of maintaining a clear image of the pelvic fin within the light sheet did not allow for PIV data to be collected during manoeuvres.

Calibration

Lateral and ventral kinematic cameras as well as the ventral PIV camera were calibrated using a three-dimensional cube-like object with 20 known point locations. Each of these points could be seen from both cameras and were digitized in both views. Using direct linear transformation the two-dimensional location of these points in both views were used to calculate the cameras location relative to each other and predict the three dimensional location of the known points [Ty Hedrick custom Matlab DLTcalibration program (Hedrick, 2008)]. This calibration allowed the calculation of three dimensional motions of the fish fins during locomotion.

To calculate fluid flow, the ventral PIV camera image was calibrated using a full field flat plate with clearly marked regularly spaced points. This image was used with DaVis software (DaVis 7.0.9, LaVision Inc., Göttingen, Germany) to correct for distortion of the camera lens and reshaped the video image to correct for parallax. All PIV videos were analyzed using corrected video images.

Electromyographic signals were synchronized using a hardwire connection from the camera trigger. In this way a single trigger determined the end time of both image collection and electromyogram signal collection allowing comparison of muscle activity with kinematics.

Anatomy and muscle stimulation

Fresh, fixed, cleared and stained specimens were used to clarify early studies of pelvic fin musculoskeletal anatomy in rainbow trout (Grenholm, 1923), similar to studies of other species (Shelden, 1937; Winterbottom, 1974).

Muscle function was assessed by stimulating *in vivo* muscle fibres in deeply anaesthetized animals. Animals were administered a lethal dose of MS-222 prior to stimulation, skin was removed from the fin area to ensure proper electrode placement. Electrodes were made from stainless steel insect pins bent to provide a surface a few millimetres long which was placed on either side of the long axis of the muscle. The aim of this placement was to stimulate the majority of the muscle at once. Because of the architecture of the pelvic girdle, only the surface muscles could be tested with certainty this way (Fig. 3). The adductor superficialis (AdS) and the extensor proprius (ExtP), located deep within the girdle were not able to be stimulated without stimulating the other muscle groups around them. Stainless steel insect pins were bent to form longer surface electrodes and held against the long axis of the surface muscles (abductor superficialis and profundus, the adductor profundus (lateral) and the infracarinalis; AbS, AbP, AdP (lateral) and Icar, respectively). These pins were connected to wires and attached to a Grass S44 electrical stimulator. Muscles were stimulated using a train of 1 ms bursts at voltage levels from 0.8 to 2.5 V and a video recording of the resultant motion of the fin was made using a Sony Digital Handycam Recorder (DCR-TRV38).

Kinematic and electromyographic measurements

Three-dimensional pelvic fin kinematics were described as the motion of each fin relative to the mid-sagittal plane and to the transverse plane [for a full description of methods refer to Standen (Standen, 2008)]. To remain consistent with Standen (Standen, 2008), in this work, adduction and abduction refer to the motion of the fin parallel to the mid-sagittal plane (or a rotation around the mediolateral axis of the fish at the fin base) whereas pronation and supination refer to the motion of the fin parallel to the transverse plane (or rotation around the cranial-caudal axis of the fish). Video sequences were three to five consecutive contra-lateral fin beats in duration and the three-dimensional motion of paired pelvic fin oscillation was quantified at 20 ms intervals.

Muscle activity was measured using size 0.002 bi-filament coated stainless steel wire (California Fine Wire Co., Grover Beach, CA, USA). Electrode tips were approximately 0.5 mm long and bent 150 deg. to create a hook. Electrodes were inserted through the skin and into the pelvic fin musculature using a 26 gauge 5/8 inch (1.5 cm)-long needle as a guide. Adductors and abductors (superficialis and profundus) were recorded during steady swimming and manoeuvres. EMG wires ran through a Grass P5 series AC pre-amplifier (Grass Technologies, Astro-Med Inc., West Warwick, RI, USA) with a band pass filter from 100 to 3000 Hz and a 5000× amplification. Data were collected at a rate of 4 kHz. EMG output was collected using Chart 5.4.2 software (ADInstruments, Colorado Springs, USA) and EMG signals were analyzed using custom Matlab programs. Raw, unfiltered EMG signals were filtered and smoothed through time-frequency decomposition using wavelet techniques (von Tscherner, 2000; Wakeling et al., 2002). A bank of wavelets

was used, with time and frequency resolution optimized for muscle, with wavelet centre frequencies ranging from 6.9 to 804.2 Hz (von Tschärner, 2000). Total myoelectric intensity was calculated at each point in time by summing intensity over wavelets with centre frequencies of 62.1–804.2 Hz removing motion artefact and electrical noise from these data. Onset and offset of EMG signals were calculated by using a threshold of two times the baseline intensity of each channel.

Describing fin motion: timing

The complex three dimensional oscillations of pelvic fins in slowly swimming trout was fully described by Standen (Standen, 2008). Fin motion is described in angles relative to the transverse and mid-sagittal planes of the fish and is plotted in polar coordinates based on the phase of the fin beat cycle. A complete fin beat cycle started with adduction at 0 deg. moved through maximal abduction at 180 deg. and returned to maximal adduction at 360/0 deg. [Fig. 4; and see figure 4 in Standen (Standen, 2008)].

During manoeuvres, no regular fin oscillation cycle exists. Manoeuvres were spontaneous yawing turns. During these turns body and fin movement patterns were divided into three stages [as in figure 8 in Standen (Standen, 2008)]: first stage started with the original body position and ended with maximum excursion of the anterior body away from the turn, second stage followed from maximum away excursion to maximum excursion of the anterior body towards the turn, finally third stage continued from maximum towards excursion to final steady body position, usually in line with the flow or slightly away from the turn.

Describing fin motion: axial coordinates

During steady swimming fish orient to the flow and swim with their dorsal side up. Axial planes oriented to the direction of flow make a good approximation of the planes that describe the fish's body. For steady swimming trials, the axial planes defined by flow direction are assumed to represent fish axial planes. The *x*-axis runs anterior to posterior along the fish. The *y*-axis runs mediolaterally from the fish's right to left side, and the *z*-axis runs dorsoventrally (Fig. 1). Data gathered in steady swimming can then be related to both fish body and flow direction simultaneously. When fish manoeuvre, however, flow direction axial planes no longer describe those fish axial planes and this is taken into consideration by creating a unique set of axes that relate both temporally and spatially to the moving fish body (see Standen, 2008).

Fin motion is described relative to two of these axial planes; the mid-sagittal and the transverse plane. Large angles between fin edge and each plane occur when the fin is fully adducted relative to the transverse plane and supinated relative to the mid-sagittal plane. Small angles, sometimes negative in the case of the mid-sagittal plane, occur when the fin is fully abducted or pronated. The magnitude of angles of fin edge relative to the mid-sagittal plane have been corrected for the contra-lateral parasagittal location of left and right pelvic fins meaning for both left and right fins large angles occur at supination and small angles at pronation.

Hydrodynamic analysis

Particle imaging velocimetry was used to visualize the flow surrounding the pelvic fins in trout. Two 8 W continuous-wave argon-ion lasers (Coherent Inc., Santa Clara, CA, USA) were focused into a single light sheet (1–2 mm thick, roughly 30 cm wide) that illuminated reflective micro particles (Vestosint polymer powder 1164, 50 µm diameter, Degussa Corp., Piscataway, NJ, USA) suspended in the flow tank. Particle movement caused by

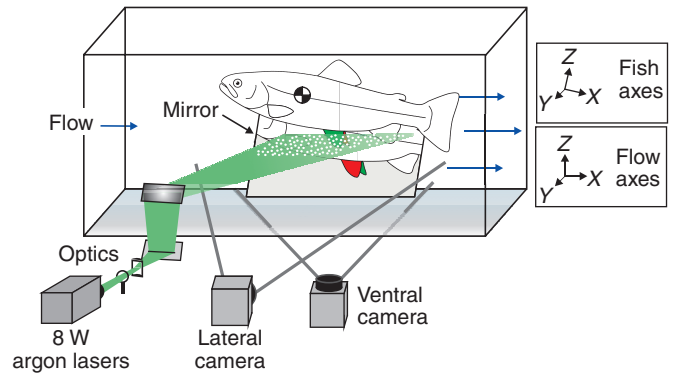


Fig. 1. Experimental apparatus. Fish swam in a multi-speed flow tank. High-speed cameras filmed ventral and lateral views simultaneously enabling three-dimensional analysis of fin motion. A mirror slightly angled along the right side of the fish allowed full visualization of the right pelvic fin. The water was seeded with neutrally buoyant particles and a horizontal laser light sheet was used to reflect off of the particles and illuminate the flow around the pelvic fins. Fin motion was measured relative to the water flow (flow axes) and relative to the fish body position (fish axes, which change as the fish turns during manoeuvres). Figure modified from figure 2 in Standen (Standen, 2008). Note that, contrary to the general axis orientation in this figure the *z*-axis increases from the dorsal to ventral aspect of the fish as described in the text and in the text of Standen (Standen, 2008). Chequered circle denotes the fish's centre of mass.

pelvic fin motion was captured by imaging the laser light sheet with a ventral high-speed video camera (Fig. 1).

Although it would have been ideal to measure flow dynamics simultaneously with EMG, the electrical noise from the laser overpowered the EMG signals making them unusable. The angle of the swimming fish, and the three-dimensional motion of the fins across two planes made it a challenge to determine complex hydrodynamic structures in the flow. Consequently, two limitations existed for the hydrodynamic analyses of this project: first, the trout were sensitive to the density of particles in the flow tank, forcing the images to be taken with a particle density lower than what would be ideal for complete hydrodynamic resolution; second, fish did not tolerate any sort of positioning when swimming at slow speeds in the flow tank, and as a result the video image could not easily be zoomed in to the pelvic fin region of the fish and was expanded to the ventral surface of the fish, in hopes of capturing the natural swimming behaviour of the animal. The larger size of the image and the lower density of particles in the flow meant that automated PIV analysis software could only be used for calculating water flow over larger areas of the animal.

A frame by frame hydrodynamic analysis was done on PIV video sequences. Flow speed and direction were calculated every 2 ms, synchronized with the kinematic analysis, providing a detailed temporal resolution of wake structure (Standen and Lauder, 2007).

Two-dimensional water velocity fields in the wake of trout were calculated from consecutive video frames (1024×1024 pixels) using DaVis 7.0.9 (LaVision Inc., Göttingen, Germany). Sequential cross-correlation was used with an initial interrogation window size of 16×16 pixels ending at 12×12 pixels (two passes with an overlap of 50%). To remove erroneous vectors, vector post processing was carried out using a median filter which removed and iteratively replaced vectors greater than 2× the root mean square of their neighbours. Horizontal plane flow fields were measured that were 226–300 cm² and contained roughly 6800 vectors (52×132 vectors). Instantaneous wake calculations were made for six different regions

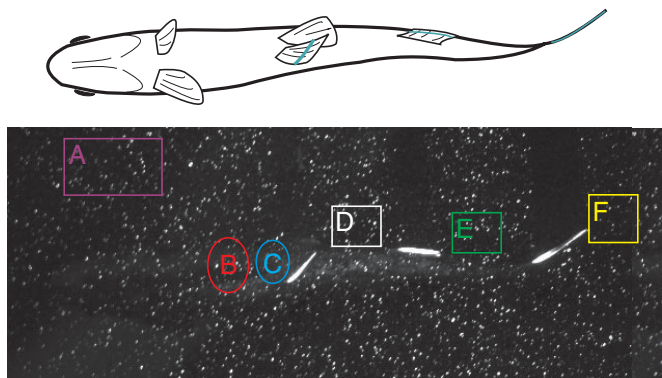


Fig. 2. Flow regions used to calculate hydrodynamic effect of pelvic fins during steady swimming. Six distinct regions of flow were analyzed to compare wake structures among fins along the ventral aspect of the fish. (A) Free stream flow (magenta); (B) pectoral, flow downstream of pectoral fins along the midline; (C) pelvic (us), flow just upstream of the pelvic fins at the midline; (D) pelvic (ds), flow taken just downstream and to the left of the left pelvic fin; (E) anal, flow taken just downstream and to the left of the anal fin; (F) tail, flow taken just downstream of the tail. Fish swam slightly tilted with their heads higher than their tails. This pitched posture sometimes led to glare from the posterior body of the fish as it neared the lightsheet. To avoid tracking the fish's body when measuring fin wakes, the posterior three regions [pelvic (ds), anal and tail] were offset to the left of the fish and therefore measured flow to the side of the oscillating fins.

along the ventral aspect of the fish (Fig. 2). Four regions were rectangular: the free stream region was located away from the fish (9.95 cm^2 , roughly 264 flow vectors) clear of any wake production to calculate the free flowing water unaltered by the fish; the pelvic (downstream) region was located just posterior of the pelvic fins and anterior of the anal fin (3.17 cm^2 , roughly 86 flow vectors); the anal region was located just downstream of the anal fin (3.62 cm^2 , roughly 96 flow vectors); and finally the tail region, located just downstream of the tail (5.49 cm^2 , roughly 143 flow vectors). To better fit the area of interest, two other regions were oval. The first oval region was located downstream of the pectoral fins (5.50 cm^2 , roughly 146 flow vectors) to calculate the magnitude of flow vectors moving ventrally along the fish's body before encountering the pelvic fins. The second region was located within the 'basket' directly in front of the pelvic fins (2.90 cm^2 , roughly 77 flow vectors), to calculate how flow changes as it encounters the pelvic fins. As the fish moved these flow regions were moved by hand to remain in the same position relative to the fish during swimming. Flow vectors contained within each region were used to calculate instantaneous flow velocities and direction through time. All variables were collected and calculated using custom Matlab programs. Flow velocity was calculated as the average magnitude of vectors within the sample ($N=77-264$ depending on region). Flow angle was calculated as the mean angle of these vectors relative to the stream-wise heading of the fish, where a zero angle was along the midline of the fish facing backward and a 180 deg. angle represented the heading of the fish.

In this study, visualization of flow was restricted to the horizontal plane. Also, the plane of oscillation of the pelvic fins made it difficult to visualize distinct vortical structures. To avoid making misleading inferences about hydrodynamic patterns caused by the pelvic fins, the analysis of flow has been simplified to a relative comparison of mean flow velocity and mean peak flow direction between the six regions described above.

Statistics

Kinematic data were analyzed according to Standen (Standen, 2008). Circular statistics were used to analyze kinematic timing data and standard statistical procedures were used to calculate mean and standard error for magnitudes of kinematic variables. Simple two-sided *t*-tests were used to compare maximum and minimum values for each variable that had equal variance and when a two-sided *F*-test determined that variables had unequal variance the Welch ANOVA was used to test for equal means (Welch, 1951).

For each muscle, EMG onset and offset timing was analyzed using basic circular statistics, like those for kinematic timing. Raleigh's tests determined if onset and offset timing was directional (occurring at a particular phase timing within the polar coordinate system rather than being randomly distributed around the polar plot) (Batschelet, 1981). Onset and offset times that had consistent (or directional) timing were compared between muscles to see if muscles were turning on and off simultaneously.

Descriptive statistics are provided for mean peak angle of flow and flow velocity for each region. Kruskal-Wallis non-parametric comparison of means was used to detect differences between mean peak flow angles (with the free stream flow subtracted), multiple comparisons were Bonferroni corrected. *t*-tests were used to compare mean flow velocities (with free stream flow subtracted) between regions (Hajek, 1969).

Significance levels for all tests were based on initial *P*-values of <0.05 and all linear statistical tests were completed using JMP (version 7.0, 2007 SAS Institute Inc., Cary, NC, USA) and Matlab. Circular statistical tests were conducted in a custom made program within Matlab (Matlab version R2006a, Mathworks, Natick, MA, USA). Measurements noted in the text are expressed as mean \pm standard error of the mean (s.e.m.). In the case of errors reported for circular statistical variables data are reported as mean \pm angular variance.

RESULTS

Fin anatomy and muscle stimulation

The pelvic girdle in rainbow trout consists of a single bony structure composed of two main parts: the basal plate and the basipterygium (Fig. 3). The basal plate is a thin, weakly ossified sheet with a robust, more highly ossified, lateral edge. The basipterygium is highly ossified on its rounded lateral edge, where it is fused with the lateral edge of the basal plate and supplies a joint surface for the pelvic fin rays. The basipterygium becomes less ossified medially and continues to be fused with the sheet of the basal plate. The left and right basal plates are joined by connective tissue and fascia at their anteriormost tips. The basipterygia are fused by a large flexible joint of connective tissue between their medial processes. A fascial plane runs along the mid-sagittal line of the fish separating left and right sides and the tips of the basal plates appear to be anchored by this fascial plane. Like most teleost fins, the pelvic fin rays are made up of dorsal and ventral hemitrichia, each pair of hemitrichia form a single, highly ossified fin ray (lepidotrichia). Each hemitrich has a shaft and a base which is bent nearly 90 deg. to the shaft. The dorsal hemitrichia seem to have a much sharper bend with a longer base compared with the ventral hemitrichia. The major muscles of the pelvic girdle originate on the basal plate and insert at the bases of the hemitrichia.

There are four major muscles that surround the pelvic girdle in rainbow trout (Fig. 3): the abductor superficialis (AbS) and profundus (AbP) and the adductor superficialis (AdS) and profundus (AdP). The abductor muscles lie ventral to the basal plate. The AbP originates on the medial half of the basal plate along its full length

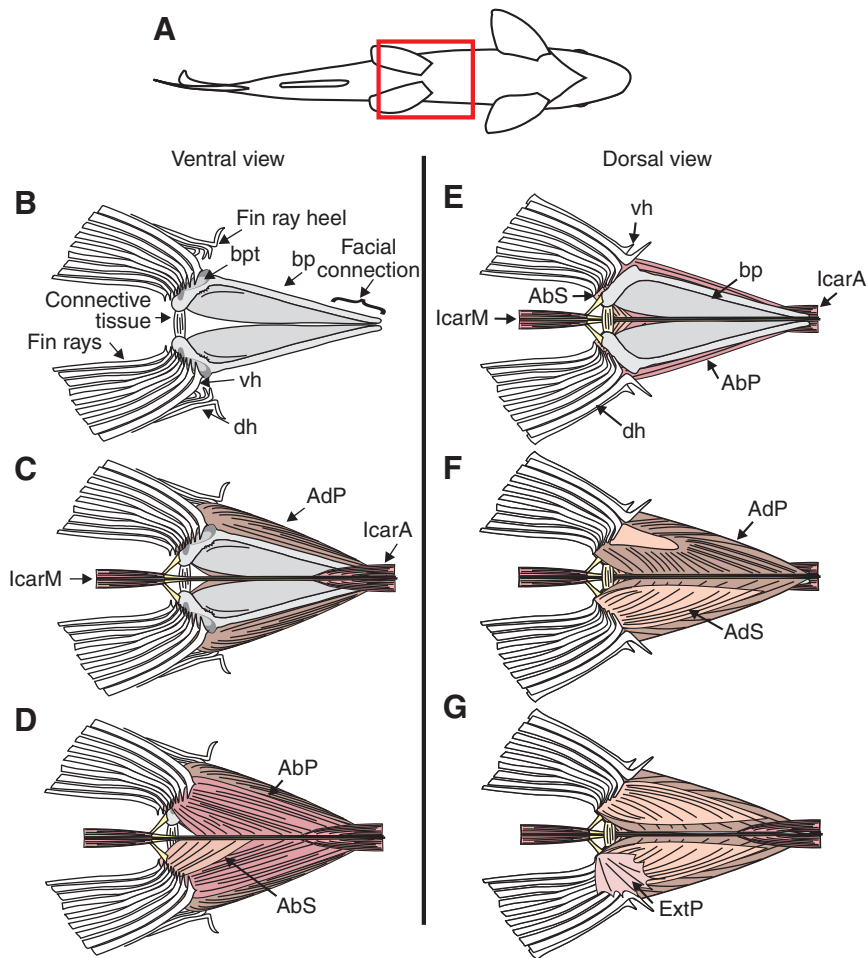


Fig. 3. Anatomy of the pelvic fins in rainbow trout. (A) Ventral view of trout. Red box denotes area of interest. (B) The bony structure of the pelvic girdle. The basipterygium (bpt) is highly ossified laterally at the articulation surface with the fin rays. Medially the two semi-ossified basal plates (bp) and the bpt are joined by connective tissue. Ventral hemitrichia (vh) and dorsal hemitrichia (dh) make up the lepidotrichia of the fin rays. (C) Infracarinalis (Icar) muscles run midline along the ventral surface of the body. The infracarinalis medius (IcarM) muscle gives way to tendons which attach both to the medial knob of the basipterygium and run medially to join with the infracarinalis anterior (IcarA). (D) The abductor superficialis (AbS) and abductor profundus (AbP) muscles originate along the midline fascia and tendon of the Icar muscles and the bp. The AbP attaches to the heel of the processes of all vh and the AbS attaches to the tips of the processes. (E) Basal plates lie dorsal to the Icar and Ab muscles. (F) The adductor profundus (AdP) originates across the dorsal side of the basal plate and along the midline fascia. This muscle is thicker on its medial and lateral edges. The adductor superficialis (AdS) lies in the cavity of the adductor profundus made by the thinning of the profundus muscle. The AbS originates on the bp through the AdP muscle. Both adductor muscles insert on the processes of the dh. (G) The extensor proprius (ExtP) is a thin sheet-like muscle originating on the heels of the medial dh and inserting into the skin and body muscle.

and inserts at the bend or heel of almost, if not all of the ventral hemitrichia. The AbS originates at the midline on the midline fascia and along the posterior medial edge of the basal plate. The AbS inserts on the tips of the attachment processes of the medial three to five ventral hemitrichia of the fin rays. The number of rays included in the AbS insertion is highly variable but consistently the two lateralmost rays are not included in the AbS insertion. Both abductor muscles also attach or originate along the fascial midline separating the two basal plates of the girdle. The adductor muscles lie dorsal to the basal plate. The AdP lies along the plate and originates at the tip and along both the lateral and medial edges of the plate. The AdP inserts on the shaft side of the heel of the bases of all dorsal hemitrichia. The AdP is a nearly bi-lobed muscle having a thickening on its medial side, thinning dramatically in the middle and thickening again laterally. This thinning creates a valley within which lies the AdS muscle. The AdS muscle originates on the basal plate and on the AdP and inserts along the bases of all but the outermost dorsal fin ray. The AdS also originates along the medial abdominal fascia.

There are three other factors that appear to influence the function of the pelvic girdle: the infracarinalis muscles (Icar), the extensor proprius muscle (ExtP), and the rotated and elongate base of the lateralmost dorsal hemitrichia. The Icar muscles run the full length of the fish, and are made up of the anterior (IcarA), medius (IcarM) and posterior (IcarP) sections. The IcarA originates on the cleithrum at the pectoral girdle and runs mid-sagittally along the belly of the fish; just anterior of the pelvic

girdle it becomes a split tendon, half of the tendon attaching and anchoring the medial process of the basipterygium and the other half continuing rectilinearly as a band of tendon attaching to the IcarM, two thirds along the length of the basal plate. This tendon provides attachment sites for abductor muscles and a sheet of fascia that runs deep along the mid-sagittal plane that divides the left and right fins. The IcarM appears somewhat entwined with the AbP at its attachment to the midline fascia. The tendinous region of the Icar appears to be attached to the mid-sagittal fascial plane, stabilizing the pelvic girdle. The ExtP is a very thin muscle, which appears to originate on the shaft side of the dorsal hemitrichia heels. Its origin is shared with the insertion of the AdS onto the dorsal hemitrichia. This delicate muscle fans laterally and attaches to the skin and body musculature at the lateral base of the pelvic fin. Finally, the lateralmost dorsal hemitrich has an elongate base and is bent 90 deg. laterally rather than medially like the rest of the rays. The only muscle attachment to this lateral bend appears to be the AdP which attaches to the shaft of the ray. The base of this ray, however, is deeply imbedded and secured within the fascial layers of the skin and body muscle.

Thus the pelvic girdle is anchored within the body of the fish by four structures: the mid-sagittal fascial plane origin of the abductors and AdP; the Icar muscles, the tendon of which incorporates itself into the mid-fascial plane; the ExtP muscle attaching the medial aspect of the fin base with the body muscle and skin; and the lateral most dorsal fin ray, also anchoring the fin with the body muscle and skin.

Table 1. Pelvic fin muscle anatomy

Muscle	Insertion	Origin	Action
Abductor profundus	Heel of all fin ray bases (ventral hemitrichia)	Along mid-sagittal fascia Ventral tip of basal plate Along medial edge of basal plate approaching tip	Medial: abducts fin Lateral: fin abduction and outer ray pronation
Adductor profundus	Heels of all fin ray bases (dorsal hemitrichia)	Along mid-sagittal fascia Dorsal side of basal plate Filaments into skin and fascia along body musculature	Lateral: outer ray pronation with mild abduction Medial: fin adduction
Abductor superficialis	Tips of medial fin ray bases (ventral hemitrichia)	Along mid-sagittal fascia Along medial edge of basal plate near the tip	Fin abduction
Adductor superficialis	Tips of medial fin ray bases (dorsal hemitrichia)	Along inner gut fascia Along mid-sagittal fascia Dorsal side of basal plate near the tip, intertwined with adductor profundus	*Direct adduction
Infracarinales	Posteroventral tip of cleithrum (pectoral girdle)	Tendon splits: half runs posteriorly along mid-sagittal line, half attaches to the medial ball of the basipterygium at fin ray bases	Stiffens mid-sagittal fascia Anchors and can move insertions of muscles attaching to fascia
Extensor proprius	Skin and body muscle	Heels of medial fin ray bases (dorsal hemitrichia)	†May control fanning of fin rays and angle of medial edge of fin relative to midline

*Unable to cleanly stimulate this muscle because of its location deep in the body of the fish. Muscle appears to function as a direct adductor.

†Unable to stimulate this muscle, function determined based on location of origin and insertion.

Muscle stimulation experiments show movement patterns of four major pelvic girdle muscles (Table 1). Stimulation of the AbP caused abduction of the fin with no fin folding or fanning. The AbS when stimulated both abducted the fin and folded it in towards the midline, minimizing surface area. Stimulation of the lateral edge of the AdP caused fin fanning and slight abduction, possibly due to bleeding of electrical current into the AbP. Stimulation of the Icar muscles stiffened the mid-sagittal fascial plane and actually changed the position of the basal plates relative to the body musculature adjusting tension of muscle fibres originating on those plates.

Kinematics and timing: steady swimming

Fish were forced to swim slowly and in so doing voluntarily swam with their bodies pitched nose up. Fish swimming at higher speeds tended to have a body angle of 0–5 deg. (E.M.S., personal observation). Body angle during swimming decreased with speed for all fish (pooled data, $\text{tilt}=36.97-17.90 \times \text{speed}$, $R^2=0.21$); mean pitch angle (measured as the angle between the longitudinal axis of the fish and the horizontal) did not significantly differ between fish (28.4 ± 4.5 deg., ANOVA, d.f.=3,9, $P=0.1186$, Tukey–Kramer HSD comparison of means $P>0.05$).

For the purposes of this paper the timing and magnitude of three variables are used to describe kinematic motion: body amplitude, fin angle with the transverse plane and fin angle with the mid-sagittal plane. A more complete description of pelvic fin kinematics has been reported previously (Standen, 2008).

Body motion was not significantly different from that reported previously (body amplitude 0.54 ± 0.03 cm, t ratio= -1.4425 , d.f.=199.9, $P=0.1507$) (Standen, 2008). Fin motion was also similar to that reported by Standen (Standen, 2008). During this study peak angles with the transverse plane were minimum 0.59 ± 0.02 rad and

maximum 0.90 ± 0.02 rad [not significantly different from Standen's data, t ratio= -1.23 (-0.74), d.f.=115.9 (122.5), $P \geq 0.2208$]; peak angles with the mid-sagittal plane were minimum -0.01 ± 0.01 rad (not significantly different from Standen's data, t ratio= -0.65 , d.f.=110.6, $P=0.5203$) and maximum 0.28 ± 0.01 rad (slightly less than Standen's data, t ratio= 2.02 , d.f.=125.0, $P=0.0457$).

The timing of each variable during the fin stroke cycle is represented using polar coordinates. As in the previous study all variables have angular directionality, meaning their maximum and minimum values occur at predictable times in the fin oscillation cycle (Rayleigh's test $P<0.0001$ for all comparisons). The timing of peak body amplitude on the fin side was not significantly different from Standen (Standen, 2008); body timing maximum excursion, fin side, $F_{(0.05(1),1,100-2)}=1.36$, $P=0.2457$. Timing of peak body amplitude on the non-fin side was slightly later compared with Standen's data (2008; 16.0 ± 13.8 deg. difference, $F_{(0.05(1),1,94-2)}=7.49$, $P=0.0074$). Maximum body excursion to the fin side occurred at 44.3 ± 13.2 deg., maximum body excursion to the non-fin side occurred roughly 180 deg. later at 237.7 ± 14.0 deg. Timing of peak fin angles relative to the mid-sagittal plane was also not different from Standen's data (max supination $F_{(0.05(1),1,254-2)}=1.829$, $P=0.1175$, max pronation $F_{(0.05(1),1,243-2)}=2.99$, $P \geq 0.0848$).

During steady swimming trout oscillated their pelvic fins relative to the transverse and mid-sagittal planes. For the purposes of this paper abduction and adduction refer to the motion of the fin relative to the transverse plane of the fish and supination and pronation refer to the motion of the fin relative to the mid-sagittal plane [see figure 4 in Standen (Standen, 2008)]. The start of the oscillation cycle was arbitrarily chosen as the point at which the lateral edge of the fin was fully adducted away from the transverse plane (Fig. 4). As the fin was abducted towards the transverse plane it supinated away from the mid-sagittal plane reaching maximum supination at roughly

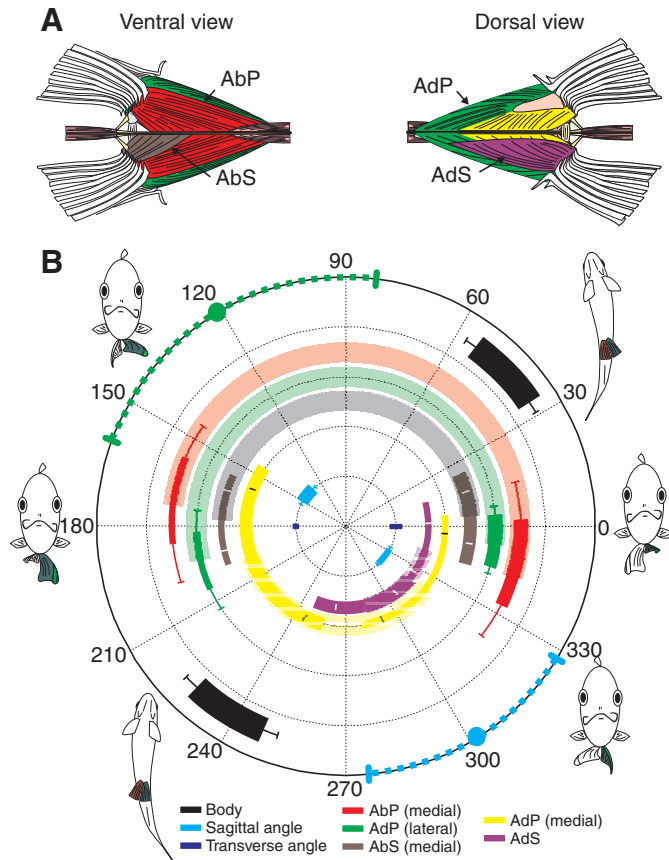


Fig. 4. Polar plot of EMG onset, offset and duration for pelvic fin musculature. (A) Diagram of pelvic fin musculature from dorsal and ventral views colour coded to match the polar plot in B. (B) Peak body amplitude (outermost circle) and pelvic fin oscillation relative to the sagittal and transverse planes (innermost circle) describe fin motion. The remaining bars represent EMG activity for all fish during all steady swimming trials. Thick bars represent mean EMG onset and thin bars represent mean offset with 95% CI, error bars represent the angular variance. Lighter bars show when muscles are active. AbP and AdP (lateral) initiate EMG activity at the start of fin abduction and stop EMG activity near the start of fin adduction. The medial AdP and the AdS, have low sample sizes (denoted by hatched bars) but appear to turn on during fin adduction and off just prior to fin abduction. Timing of mean maximum flow angle is indicated with a green circle and mean minimum flow angle is indicated with a blue circle, with dotted lines representing angular variance.

132 deg. (mean phase angle 132.4 ± 18.8 deg., $N=159$, $P < 0.0001$). The fin began pronating while continuing to abduct until mid-stroke (180 deg.). Fin adduction began while the fin continued pronating, reaching maximum pronation at roughly 316 deg. (mean phase angle 316.5 ± 21.3 deg., $N=151$, $P < 0.0001$). Finally as supination began again, the fin became fully adducted and began the next fin beat cycle (0 deg./360 deg.). Left and right fins did not differ in relative timing of peak angles with the mid-sagittal plane (pronation, $F_{(0.05(1), 1, 245-2)} = 2.99$, $P = 0.0848$; supination, $F_{(0.05(1), 1, 256-2)} = 1.829$, $P = 0.1775$) but oscillated roughly 180 (175.7 ± 7.99) deg. out of phase with each other; this means when the left fin was maximally abducted towards the transverse plane the right fin was maximally adducted.

Fin kinematics: manoeuvres

Slow-speed steady swimming in trout is accompanied by remarkably predictable and regular pelvic fin oscillations (Fig. 5). By contrast yawing manoeuvres show large temporal variation in pelvic fin

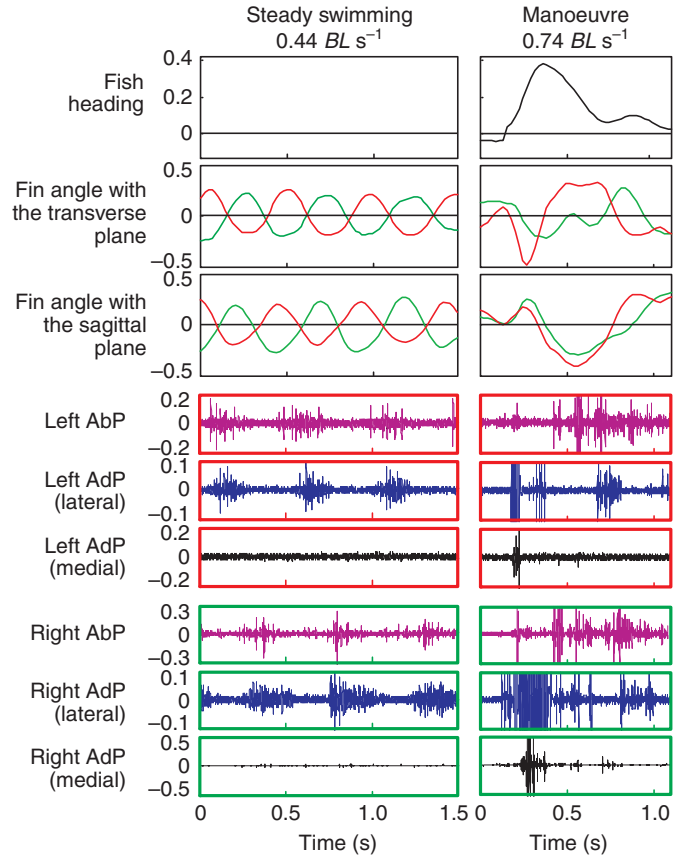


Fig. 5. Pelvic fin kinematics and muscle activity. Raw EMG signals and corresponding fish heading and fin motion during steady swimming and manoeuvres in trout. Red lines represent motion of right fin and green lines represent motion of left fin. During steady swimming regular oscillatory motions of fins correspond with regular muscle activity patterns in abductor profundus (AbP), and lateral adductor profundus (AdP). The medial portion of the AdP is active only during manoeuvres and not during steady swimming. EMG signals during manoeuvres operate at high intensity and therefore go beyond the relative axes of the figure (original recordings were not clipped).

motion (Fig. 5). Kinematic data for yawing manoeuvres are taken from Standen (Standen, 2008) and are primarily used to show the proper electrode placement in muscles not active during steady swimming. A brief comparison of manoeuvres with steady swimming is also included in this paper.

Electromyogram activity

For the purposes of this study EMG was used as a measure of when the fin muscles were active (turned on) and inactive (turned off). Consistent measures of AbP (medial), AbS, AdP (lateral) and AdP (medial) were made across fish. Although only available in one fish, measurements from the AdS were also made (Table 2).

For all fish, during steady swimming, the AbP (medial) and AdP (lateral) were active during fin abduction towards the transverse plane (left fin AbP onset occurring at 347.9 ± 26.9 deg. and offset occurring at 171.9 ± 26.9 deg., left fin AdP onset occurring at 354.6 ± 13.0 deg. and offset at 193.9 ± 20.0 deg.; right fin AbP onset occurring at 41.1 ± 19.1 deg. and offset occurring at 269.2 ± 42.2 deg., right fin AdP onset occurring at 29.0 ± 19.6 deg. and offset at 190.1 ± 16.4 deg.; all Raleigh's tests, significant $P \leq 0.0094$). The three other muscles measured had variable activity patterns during steady

Table 2. Electromyogram electrode placement and signals

Pelvic fin muscle	Number of fish	Left fin	Right fin	Activity	Speed (BL s ⁻¹)	Tilt (deg.)
Abductor profundus (medial)	3	3	1	Strong consistent	0.2–0.74	5.2–44.2
Abductor superficialis	3	1	2	Strong consistent	0.2–0.96	5.2–44.2
Adductor profundus (lateral)	4	4	4	Strong consistent	0.2–0.96	5.2–44.2
Adductor profundus (medial)	4	1	3	Weak inconsistent or not active	0.2–0.96	5.2–44.2
Adductor superficialis	1	1	0	Weak inconsistent or not active	0.24–0.96	25.8–34.7

'Weak' suggests the muscle is active but at a very low intensity. 'Inconsistent' suggests muscle is active but not in a predictable way. 'Not active' suggests the electrode is well placed but the muscle is not always used.

swimming. This means that not all fish activated these muscles and when they were activated they were not consistent between fins or beats. When used, the AbS (medial) was active during fin abduction (left fin onset=4.5±12.6 deg. left fin offset=178.0±15.3 deg.; right fin onset=333.8±16.7 deg. right fin offset=184.3±16.9 deg.); the AdP (medial) was active during adduction (left fin onset=202.3±43.4 deg. left fin offset=323.1±32.4 deg.; right fin onset=83.9±3.2 deg. right fin offset=152.7±2.7 deg.); and the AdS was active briefly during the last part of adduction away from the transverse plane (left fin onset=284.6±21.8 deg. left fin offset=343.7±17.6 deg.; right fin not measured).

Hydrodynamics of pelvic fins

Flow angle in the pectoral region did not oscillate with the same predictability as the more posterior regions (Fig. 6; see Fig. 2 for region location). Peak mean flow angle was higher in all regions compared with the free stream flow (Tables 3, 4; $\chi^2=945.26$, $P<0.0001$) suggesting all fins contributed lateral swimming forces (freestream flow angle ~0 deg.). Although the peak mean flow angle did not differ between pectoral and pelvic (us) regions, peak mean flow angles decreased posteriorly [pelvic (ds)>anal>tail]. This pattern again suggests a dichotomy of fin function: the paired anterior fins brake and stabilize while the posterior median fins accelerate and stabilize.

Flow angle in the wake of the pelvic fin [pelvic (ds)] reached its maximum (170.0 deg. flow angle, mean flow subtracted) just before midstroke at 121.9±38.5 deg. through the stroke cycle, and reached its minimum (133.6 deg. flow angle, mean flow subtracted) at 301.4±26.1 deg. through the stroke cycle (Fig. 4).

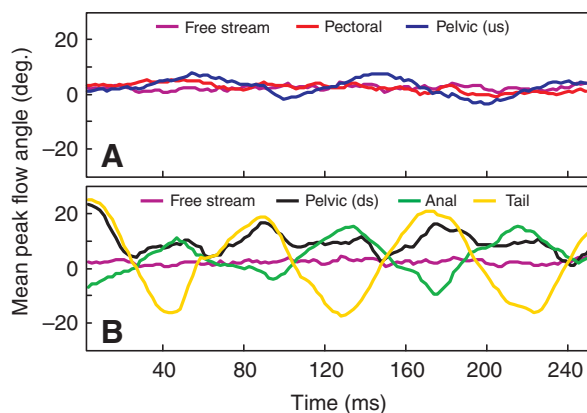


Fig. 6. Mean peak flow angle for different regions along steadily swimming fish. (A) Free stream flow compared with pectoral and pelvic (us) regions; very little regular oscillation in mean peak angle is evident. (B) Free stream flow compared with pelvic (ds), anal and tail regions. Regular oscillation in flow angle can be seen developing around the pelvic region and building towards the tail. See Fig. 2 for region location.

Mean flow velocity (downstream and lateral) varied between regions (Tables 3, 5, Fig. 7). The pectoral and pelvic (ds) regions had lower velocity downstream flow than the free stream ($P<0.013$). The anal region did not differ in downstream flow from the free stream ($P=0.0639$) and the tail region had a higher downstream flow compared with the free stream ($P=0.0034$). This suggests the anterior fins of the fish are acting to slow flow by producing drag wakes while the posterior median fins appear to be contributing thrust to the ventral flow. With the exception of the pectoral region all other regions have higher lateral flow velocities than free stream ($P<0.0014$) suggesting all fins make a contribution to the stabilizing forces acting on the fish's body. Although the pelvic (ds) and anal regions produce the same velocity of lateral flow during oscillation, downstream and lateral flow velocity produced by fins increases posteriorly ($P<0.0281$).

DISCUSSION

This paper uses electromyography and particle imaging velocimetry to test the hypotheses set forth in Standen (Standen, 2008) and determines that paired pelvic fins are actively moved and produce hydrodynamic forces during steady swimming and manoeuvres in trout.

Observed muscle function

Pelvic fin musculature was active both during steady swimming and manoeuvres. Of interest, both abductors (Ab) and adductors (Ad) were active simultaneously. Deep medial abductors (AbP) activated at the start of fin abduction as expected, abducting the fin. Deep lateral adductors (AdP lateral) were also active during fin abduction. In isolated stimulation experiments, the AdP (lateral) pulled on the outside of the shafts of the lateral most fin rays, fanning out the outermost fin rays. Activation of the AdP (lateral) muscle

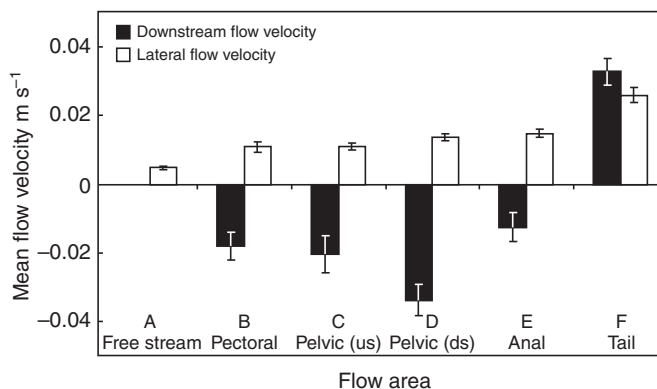


Fig. 7. Mean flow velocity for different regions along steadily swimming trout. Mean freestream flow (\pm s.e.m.) in the downstream direction has been subtracted from each flow region. Data averaged over all fish and all steady swimming trials ($N=10$).

Table 3. Mean peak flow angle and mean flow velocity at different regions along steadily swimming fish

Flow region	N (peak angle)	With mean	Mean free	N (flow velocity)	Mean free	Mean lateral flow velocity [†] (m s ⁻¹)
		free stream flow	stream flow subtracted		stream flow subtracted	
		Mean peak angle (deg.)	Mean peak angle (deg.)		Mean downstream flow velocity (m s ⁻¹)	
Free stream	2478	1.27±0.1	n.a.	20	0	0.0047
Pectoral fins	66	30.93±5.9	147.6±3.9	20	-0.018	0.011
Pelvic fins (upstream)	62	13.06±2.8	153.9±3.0	20	-0.020	0.011
Pelvic fins (downstream)	63	33.84±2.4 [-11.83±11.2]*	170.0±1.1 [133.62±26.6]*	20	-0.034	0.014
Anal fin	59	19.00±1.0	153.9±3.2	20	-0.013	0.015
Tail	32	24.23±1.3	55.7±3.0	10	0.033	0.026

The mean of the free stream region is calculated from all data points because the free stream flow is regular and uniform with no clear oscillations from which to collect peak flow.

*Angles in square brackets represent minimum peak angles for the pelvic fin downstream region. All other mean peak flow angles represent maximum peak flow values.

[†]Mean lateral flow velocity is calculated as the absolute value of the flow in the lateral direction. Because lateral velocity oscillated between positive and negative values taking the absolute value avoids the error caused by calculating a mean velocity of zero. Averaging the absolute value over time underestimates the true lateral velocity of the flow but due to a lack of consistent oscillations in velocity, peak values could not be reliably sampled.

Table 4. Statistical comparison of mean peak flow angle at different points along steadily swimming fish

Flow region one	Flow region two	Degrees of freedom	χ^2	P-value
A: Free stream	All other regions (B,C,D,E,F)	5,2837	945.26	0
B: Pectoral fin	C: Pelvic fin (up stream)	1,153	0.33	0.5672
D: Pelvic fin (down stream)	E: Anal fin	2,202	137.5	0
D: Pelvic fin (down stream)	F: Tail fin			
E: Anal fin	F: Tail fin			

Kruskall–Wallis non-parametric comparison of mean peak angles (mean free stream flow subtracted), Bonferonni corrected for multiple comparisons.

at the same time as the medial AbP resulted in an abduction and supination of the fanned fin. The AbP supplied resistance to the AdP (lateral) so that when the adductor contracted it held the fin surface fanned out while it was being abducted.

Although the neuroanatomical pathways of the pelvic fins have not been described, work on dorsal and caudal fin motor enervation suggests fish fin musculature is innervated by multiple motor neurons (Schneider and Sulner, 2006). Although subtle control of muscle contraction can be achieved by modulating the firing rate and timing of action potentials in a single motor nerve, if each pelvic fin muscle is enervated by multiple motor neurons, greater control of both contraction intensity and duration could be altered over the fin beat cycle. Modulating the intensity of simultaneously contracting AdP and AbP would allow for a smooth transition

between abduction and supination, followed by adduction and pronation of the fin surface. Varying intensity of each contracting muscle controls the amount of abduction relative to pronation affected by the fin. Based on the angle of the muscles relative to the fin surface, and the 90 deg. lateral bend in the outermost fin ray anchored in the skin, with appropriate muscle modulation, it appears the contralateral oscillation of the pelvic fins could be driven by these two muscles alone. Measurements taken on a sample specimen suggest the fascicle length of the AbP is longer than that of the AdP (roughly 11.32 and 9.03 mm, respectively). The mass of these muscles differs slightly as well, the AbP being slightly larger than the AdP (roughly 0.042 and 0.037 g, respectively). Although taken on fixed tissue which may have affected mass and length, these measurements suggest that the AbP and AdP are capable of

Table 5. Statistical comparison of mean flow velocity at different points along swimming fish

Flow region one	Relative downstream flow velocity (m s ⁻¹)	Relative lateral flow velocity (m s ⁻¹)	Flow region two	P-value downstream velocity	P-value [‡] lateral velocity
Free stream	>	=	Pectoral	0.013*	0.0519
	=	<	Pelvic (upstream)	0.269*	0.0014
	>	<	Pelvic (downstream)	0.0005*	0
	=	<	Anal	0.0639*	0.0001
	<	<	Tail	0.0034*	0.0011
Pectoral	=	=	Pelvic (upstream)	0.7139 [†]	0.9618
Pelvic (downstream)	<	=	Anal	0 [†]	0.2696
Pelvic (downstream)	<	<	Tail	0.0007 [†]	0.0073
Anal	<	<	Tail	0.0013 [†]	0.0281

All velocities used in the comparison had the mean free stream velocity subtracted. *Comparisons with free stream flow in the downstream direction were made by testing the resultant value for that region against zero. [†]All other comparisons were done by subtracting flow region two from flow region one and testing the resultant value against zero. [‡]Calculations for comparisons of flow in the lateral direction were made using absolute values.

producing similar forces (10.5 and 11.6 N, respectively, using vertebrate muscle densities of 1.06 g cm^{-3} and maximum isometric stress of vertebrate skeletal muscle of 0.3 MPa).

Additional subtle control of fin motion may be the result of the ‘floating’ nature of the pelvic girdle. The pelvic girdle is not attached to the axial skeleton and is supported entirely by fascia and muscle. The additional fin musculature (Icar and ExtP, see Fig. 3) acts to stabilize and anchor the pelvic girdle. These muscles may also change the location and stiffness of the floating pelvic girdle. This could affect the angle of action of each muscle, subtly changing the mechanical effect or function of the adductor and abductor muscles to control the motions of the fin.

Although there is not an arrector muscle associated with the trout pelvic fin (Grenholm, 1923), the AdP is bi-lobed and appears to be functionally partitioned along its mediolateral axis. Locomotory muscles in mammals can be recruited compartmentally along their long axis (Wakeling et al., 2007; Wakeling, 2009) which makes it reasonable to think the AdP muscle of the pelvic fin is being recruited compartmentally along its width. Only the lateral component of the AdP is active during steady swimming. The medial component remains inactive until manoeuvres require recovery from large fin abductions. For example in Fig. 5 the right AdP (medial) is active during a large adduction which returns the fin toward the body after a significant manoeuvring abduction. This ability for the AdP to be selectively activated along its mediolateral axis allows the lateral portion of the muscle to act as an arrector.

Hydrodynamic fin function

The flow patterns along the ventral aspect of the swimming fish can help determine the function of fins along that surface. Pelvic fins in trout are located half way along the long axis of the fish and therefore affect flow along a large portion of the fish’s body. Quantifying flow in several areas along the fish’s belly shows that pelvic fins could produce two hydrodynamic effects: (1) slowing flow and (2) production of lateral forces.

Contra-lateral pelvic fin oscillation occurs only when fish swim at slow speeds. Unlike derived actinopterygian fishes such as the surfperch (Drucker, 1996; Drucker and Jensen, 1996), when trout swim at slow speeds they continue to beat their tails. Two things appear to occur during caudal oscillation at slow swimming speeds. First, the caudal fin produces more thrust than is necessary to hold station in slow flows. Trout counteract this thrust by pitching nose up, increasing body area presented to the flow and thus increasing the resultant drag. Second, even though the tail is producing more thrust than it needs to hold station in slow flow, the thrust forces are so low at these speeds that the ratio of lateral tail force production to downstream tail force production appears to increase with decreasing swimming speed as seen in studies of caudal fin wake in fishes swimming at different speeds (Nauen and Lauder, 2002). The relative increase in lateral forces produced by the tail along with the pitched body position places the tail well behind and below the fish’s centre of mass creating a moment arm for the tail that could influence pitch, roll and yaw destabilizing the fish during slow speed swimming.

The location of the pelvic fins well behind the fish’s centre of mass make them ideal for controlling body pitch and yaw. During this study, flows recorded both in front and behind the pelvic fins showed fins are slowing flow along the body. The reduction in flow at the pelvic fins means they are producing drag forces behind and below the centre of mass, this will provide torques to reduce head-up pitch and side-to-side yaw as well as to slow forward swimming speed, supporting the hypothesized function of these fins calculated

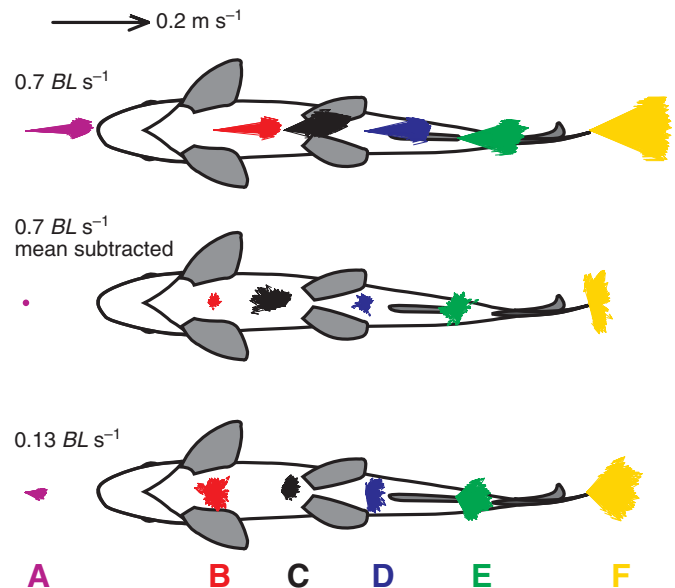


Fig. 8. Relative contribution of ventral flow at two different swimming speeds in trout. Mean flow angle of different regions represented by flow vectors of corresponding colour. Each individual arrow represents the average flow vector for that region for a given point in time. Several seconds of data are represented in this figure to show the variation in flow direction throughout several fin beats. (Top fish) Mean flow angle of the different regions for fish swimming at 0.7 BL s^{-1} . (Middle fish) Mean flow angle for the same sequence as the top fish with mean free stream flow subtracted. (Bottom fish) Mean flow angle including free stream flow, for the same fish swimming at 0.13 BL s^{-1} .

from kinematics by Standen (Standen, 2008). Pectoral fins also appear to provide a stabilizing function. Although located ahead of the centre of mass, pectoral fins appear to produce predominantly lateral wakes, suggesting a corrective force producing function. Similar findings were made by Drucker and Lauder (Drucker and Lauder, 2003) during fin protraction while hovering, in trout. Often the lateral forces produced by the paired fins do not oscillate with a regular motion, suggesting paired fins are fine tuning body position by producing lateral forces when needed.

The general pattern of flow along the ventral region of the fish suggests downstream flow velocity decreases as it moves from the snout towards the pelvic fins. Flow velocity increases again as it encounters the anal fin and tail. This initial slowing and then accelerating of flow along the fish’s belly suggests different functions of anterior *versus* posterior ventral fins (Fig. 8). At particularly slow swimming speeds, the fish balance body and posterior fin thrust producing motions with braking paired fin motions to maintain swimming speed, suggesting that this is a bioenergetically expensive swimming behaviour because of the simultaneous production of both drag and thrust (Webb, 2006).

Pelvic fin functional significance

Rotational disturbances present large control problems for swimming fish (Eidietis et al., 2002; Webb, 2002; Webb, 2004). In addition, rotational perturbations are more likely to be amplified than translational perturbations (Hoerner, 1975). Based on their position posterior and ventral to the fish’s centre of mass, pelvic fins can produce considerable rotational torque in pitch, roll and to some extent yaw (Weihs, 2002). Regardless of what type of forces pelvic

fins produce (drag or lift based) their location relative to the centre of mass makes them important for body stabilization during locomotion.

It has been suggested that pelvic fin wakes influence the hydrodynamic performance of anal fins (Standen and Lauder, 2007). Pelvic fin wakes may change the angle of attack of the anal fin allowing it to shed lateral jets earlier than expected, balancing forces produced by the dorsal fin. There is no doubt from this study that pelvic fins alter the flow encountered by the anal fin given that the pelvic fin wake is significantly different from the free stream flow. In fact, pectoral fins significantly alter flow direction along the belly of the fish (Table 4), and they do so in an irregular, non-oscillatory pattern (Fig. 6). Pelvic fins appear to organize the ventral flow into a regular oscillation cycle affecting the flow direction encountered by the anal fin. As predicted by Standen and Lauder (Standen and Lauder, 2007), the pelvic fin wake alters the flow around the anal fin and may influence the timing of jets released by the anal fins.

Although, from kinematic analysis of certain parts of their oscillation cycle, it appears that pelvic fins may act as dihedral foils, statically stabilizing the fish by holding themselves rigid against oncoming flow, it is impossible to prove this hypothesis with the current PIV analysis techniques. PIV analysis is excellent for visualizing large wake structures where fluid is actively moved, however, subtle boundary layer effects are difficult to visualize on a moving structure (Anderson et al., 2001). What can be seen from this study is that the jet angle is closest to 180 deg. (or flowing upstream) mid way through fin abduction as was hypothesized by Standen (Standen, 2008) and the lateral-most facing jet occurs near maximum fin pronation when the fish's body is accelerating through to reach maximum excursion to the fin side. Based on these flow patterns it appears that the pelvic fins act to dampen the oscillation of the body within the stroke cycle.

ACKNOWLEDGEMENTS

Thanks to G.V. Lauder and members of his laboratory for valuable discussions and ideas during the course of this paper, and to two anonymous reviewers who made valuable suggestions. I am grateful as well to Whitney Kress, for her patience and skill in digitizing and her enthusiasm for learning how to analyze EMG signals. Thanks to the wonderful fish care folks, Tony Julius and Willy Goldsmith. Grateful thanks also to master programmers Ty Hedrick and Eric Tytell for the use of their DLDataviewer and analyzePIV programs, respectively. For ideas, inspiration and general education thanks to Karel F. Leim, Monica Daly, Tim Higham, Chris Richards and Marcus Roper. Finally, thanks to Wayne Miller from Blue Stream Trout Hatchery who generously provided beautiful trout who swam wonderfully despite duress. Funding for this research was provided by NSERC to E.M.S. and by NSF IBN0316675 to George V. Lauder, Harvard University.

REFERENCES

- Anderson, E. J., McGillis, W. R. and Grosenbaugh, M. A. (2001). The boundary layer of swimming fish. *J. Exp. Biol.* **204**, 81-102.
- Batschelet, E. (1981). *Circular Statistics in Biology*. New York: Academic Press.
- Drucker, E. G. (1996). The use of gait transition speed in comparative studies of fish locomotion. *Am. Zool.* **36**, 555-566.
- Drucker, E. G. and Jensen, J. S. (1996). Pectoral fin locomotion in the striped surfperch. 2. Scaling swimming kinematics and performance at a gait transition. *J. Exp. Biol.* **199**, 2243-2252.
- Drucker, E. G. and Lauder, G. V. (2003). Function of pectoral fins in rainbow trout: behavioral repertoire and hydrodynamic forces. *J. Exp. Biol.* **206**, 813-826.
- Drucker, E. G. and Lauder, G. V. (2005). Locomotor function of the dorsal fin in rainbow trout: kinematic patterns and hydrodynamic forces. *J. Exp. Biol.* **208**, 4479-4494.
- Eidietis, L., Forrester, T. L. and Webb, P. W. (2002). Relative abilities to correct rolling disturbances of three morphologically different fish. *Can. J. Zool.* **80**, 2156-2163.
- Goto, T., Nishida, K. and Nakaya, K. (1999). Internal morphology and function of paired fins in the epaulette shark, *Hemiscyllium ocellatum*. *Ichthyological Research* **46**, 281-287.
- Grenholm, A. (1923). *Studien über die flossenmuskulatur der teleostier*. Uppsala: Uppsala universitets arsskrift.
- Hajek, J. (1969). *A Course in Non-parametric Statistics*. San Francisco: Holden-Day.
- Hale, M. E., Day, R. D., Thorsen, D. H. and Westneat, M. W. (2006). Pectoral fin coordination and gait transitions in steadily swimming juvenile reef fishes. *J. Exp. Biol.* **209**, 3708-3718.
- Harris, J. E. (1937). The mechanical significance of the position and movements of the paired fins in the Teleostei. In *Papers from Tortugas Laboratory*, vol. 16, pp. 173-189. Carnegie Institution of Washington, DC.
- Harris, J. E. (1938). The role of the fins in the equilibrium of the swimming fish. II. The role of the pelvic fins. *J. Exp. Biol.* **15**, 32-47.
- Hedrick, T. L. (2008). Software techniques for two- and three-dimensional kinematic measurements of biological and biomimetic systems. *Bioinspir Biomim* <http://stacks.iop.org/1748-3190/3/034001>, 034001.
- Hoerner, S. F. (1975). *Fluid-Dynamic Lift*. Hoerner Fluid Dynamics, Brick Town, NJ: Mrs Liselotte A. Hoerner.
- Kawabe, R., Kawano, T., Nakano, N., Yamashita, N., Hiraishi, T. and Naito, Y. (2003). Simultaneous measurement of swimming speed and tail beat activity of free-swimming rainbow trout *Oncorhynchus mykiss* using an acceleration data-logger. *Fisheries Science* **69**, 959-965.
- Monoyer, F. (1866). Recherches expérimentales sur l'équilibre et la locomotion chez les poissons. *Ann. Sci. Nat.* **5**, 5-15.
- Nauen, J. C. and Lauder, G. V. (2002). Hydrodynamics of caudal fin locomotion by chub mackerel, *Scomber japonicus* (Scombridae). *J. Exp. Biol.* **205**, 1709-1724.
- Peng, J., Dabiri, J. O., Madden, P. G. and Lauder, G. V. (2007). Non-invasive measurement of instantaneous forces during aquatic locomotion: a case study of the bluegill sunfish pectoral fin. *J. Exp. Biol.* **210**, 685-698.
- Pridmore, P. A. (1994/95). Submerged walking in the epaulette shark *Hemiscyllium ocellatum* (Hemiscyllidae) and its implications for locomotion in rhipidistian fishes and early tetrapods. *Zoology* **98**, 278-297.
- Schneider, H. and Sulner, B. (2006). Innervation of dorsal and caudal fin muscles in adult zebrafish *Danio rerio*. *J. Comp. Neurol.* **497**, 702-716.
- Shelden, F. F. (1937). Osteology, myology and probable evolution of the nematognath pelvic girdle. *Ann. NY Acad. Sci.* **37**, 1-96.
- Standen, E. M. (2008). Pelvic fin locomotor function in fishes: three-dimensional kinematics in rainbow trout (*Oncorhynchus mykiss*). *J. Exp. Biol.* **211**, 2931-2942.
- Standen, E. M. and Lauder, G. V. (2007). Hydrodynamic function of dorsal and anal fins in brook trout (*Salvelinus fontinalis*). *J. Exp. Biol.* **210**, 340-356.
- Tytell, E. D., Standen, E. M. and Lauder, G. V. (2008). Escaping flatland: three-dimensional kinematics and hydrodynamics of median fins in fishes. *J. Exp. Biol.* **211**, 187-195.
- von Tscherner, V. (2000). Intensity analysis in time-frequency space of surface myoelectric signals by wavelets of specified resolution. *J. Electrom. Kin.* **10**, 433-445.
- Wakeling, J. M. (2009). The recruitment of different compartments within a muscle depends on the mechanics of the movement. *Biol. Lett.* **5**, 30-34.
- Wakeling, J. M., Kaya, M., Temple, G. K., Johnston, I. A. and Herzog, W. (2002). Determining patterns of motor recruitment during locomotion. *J. Exp. Biol.* **205**, 359-369.
- Wakeling, J. M., Rituechai, P., Dalton, S. and Nankervis, K. (2007). Segmental variation in the activity and function of the equine longissimus dorsi muscle during walk and trot. *Equ. Comp. Ex. Phys.* **4**, 95-103.
- Webb, P. W. (1971a). The swimming energetics of trout. II. Oxygen consumption and swimming efficiency. *J. Exp. Biol.* **55**, 521-540.
- Webb, P. W. (1971b). The swimming energetics of trout. I. Thrust and power output at cruising speeds. *J. Exp. Biol.* **55**, 489-520.
- Webb, P. W. (2002). Control of posture, depth, and swimming trajectories of fishes. *Integr. Comp. Biol.* **42**, 94-101.
- Webb, P. W. (2004). Response latencies to postural disturbances in three species of teleostean fishes. *J. Exp. Biol.* **207**, 955-961.
- Webb, P. W. (2006). Stability and maneuverability. In *Fish Biomechanics*, vol. 23 (ed. R. E. Shadwick and G. V. Lauder), pp. 281-332. San Diego: Elsevier.
- Weih, D. (2002). Stability versus maneuverability in aquatic locomotion. *Integr. Comp. Biol.* **42**, 127-134.
- Weich, B. L. (1951). On the comparison of several mean values: an alternative approach. *Biometrika* **38**, 330-336.
- Wilga, C. D. and Lauder, G. V. (2004). Biomechanics of Locomotion in Sharks, Rays and Chimeras. In *Biology of Sharks and their Relatives* (ed. J. C. Carrier J. A. Musick and M. R. Heithaus), 616pp. Washington, DC: CRC Press.
- Winterbottom, R. (1974). Descriptive synonymy of the striated muscles of the Teleostei. *P. Acad. Nat. Sci. Phila.* **125**, 225-317.